DOI: 10.1002/ejic.201000381

Tetranuclear Manganese Complexes with $[Mn^{II}_4]$ and $[Mn^{II}_2Mn^{III}_2]$ Units: Syntheses, Structures, Magnetic Properties, and DFT Study

Lucjan B. Jerzykiewicz,[a] Józef Utko,[a] Marek Duczmal,[b] Przemysław Starynowicz,[a] and Piotr Sobota*[a]

Dedicated to Professor Stanislaw Pasynkiewicz on the occasion of his 80th birthday

Keywords: Manganese / Metal alkoxides / Synthetic methods / X-ray diffraction / Magnetic properties

Two tetranuclear manganese compounds, $[Mn_4(\mu_3,\eta^2\text{-}L)_4Br_4(LH)_4]$ (**1**) and $[Mn_4(\mu_3,\eta^2\text{-}L)_2(\mu,\eta^2\text{-}L)_4L_2Br_2]$ (**2**), with cubane and defect dicubane-like cores were synthesized and characterized by single-crystal X-ray diffraction, magnetic measurements, and DFT calculations (LH = 2-methoxyethanol). The magnetic properties of the resulting $[Mn_4]$ building blocks are presented and discussed in detail. In particular, in **2** the Mn^{III}–O–Mn^{III} angle 103.12(8)° is the largest observed to date for such a system. The conjunction of antiferromagnetic and ferromagnetic interactions within the tetranuclear mixed-valent $Mn^{II}_2Mn^{III}_2$ complexes results in an unusual S_T = 1 ground state.

Introduction

In the last few years, many classes of tetranuclear manganese compounds with various oxidation states and geometries have been prepared and studied.[1] Among these complexes, cube $[Mn_4(\mu_3\text{-}O)_4]$ and defect dicubane-like $[Mn_4(\mu_3\text{-}O)_2(\mu\text{-}O)_4]$ cores are very important due to their biological functions such as the active centers of photosynthetic water oxidation and their single molecule magnet (SSM) behavior.[2] Development and optimization of preparative routes towards the synthesis of polynuclear Mn complexes is thus of great interest not only for the discovery of completely new complexes but also as a way of building up families of related species so that structure–property relations can be developed.[3] We have previously described a simple and efficient self-assembly method for the in situ generation of cuboidal complexes.[1g] In the present work we describe the synthesis, structure, and magnetic properties of two different tetranuclear Mn clusters with Mn^{II}_4 and $Mn^{II}_2Mn^{III}_2$ systems.

Results and Discussion

Syntheses

A general synthetic route for manganese complexes used in this study is shown in Scheme 1. The reaction of metallic Mn powder with 2-methoxyethanol (LH) in the presence of NH_4Br in toluene under reflux yielded a dark-brown slurry, which after filtration was left for crystallization at room temperature. After a few days, colorless crystals of $[Mn_4(\mu_3,\eta^2\text{-}L)_4Br_4(LH)_4]$ (**1**, 62%) were collected by filtration. Next, the filtrate was concentrated and left again for crystallization to give red crystals of $[Mn_4(\mu_3,\eta^2\text{-}L)_2$-

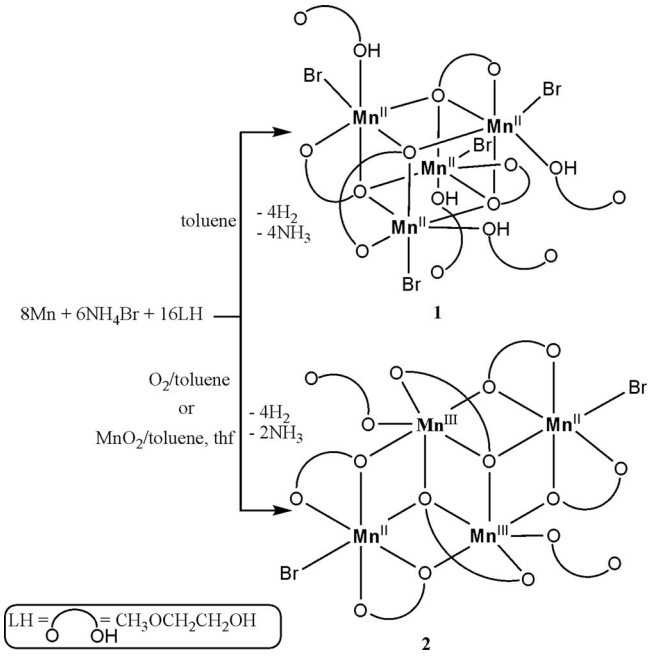

Scheme 1. Synthesis of **1** and **2**.

[a] Faculty of Chemistry, University of Wrocław,
14 F. Joliot-Curie, 50-383 Wrocław, Poland
Fax: +48-71-328-2348
E-mail: plas@wchuwr.pl
[b] Faculty of Chemistry, Wrocław University of Technology,
27 Wyspiańskiego, 50-370 Wrocław, Poland

Supporting information for this article is available on the WWW under http://dx.doi.org/10.1002/ejic.201000381.

$(\mu,\eta^2\text{-}L)_4L_2Br_2]$ (**2**) in 8% yield. Furthermore, an increased yield of **2** (29%) was achieved when the reaction was carried out in the presence of a stoichiometric amount of MnO_2. NH_4Br plays an important role in the synthesis of these compounds as a factor enabling the activation of the metal surface and oxidation of Mn to Mn^{II} by H^+ and as the source of Br^- ions, which act as terminal ligands in the compounds. It is worth mentioning that the use of NH_4Cl instead of NH_4Br leads to the formation of the $Mn^{II}_4(\mu\text{-}Cl)_2\text{-}Mn_4^{II}$ unit, created by double chloride linkage of the two Mn_4^{II} cubanes.[1g]

Description of Structures

Complex **1** is composed of four manganese, four bromide, and four 2-methoxyethanolate ions, as well as four methoxyethanol molecules (Figure 1). The manganese(II) ions and bridging alkoxido groups are arranged in a cubane core, which is stabilized by relatively strong intramolecular O–H···Br hydrogen bonds formed between the manganese bonded Br ion and the OH group of the alcoholic ligand. The H atom of this bond lies in the plane of the MnOBrMn fragment. Distortion of the core from a perfect cube, characteristic for the $[Mn_4(\mu_3\text{-}O)_4]$ cuboidal fragment is conspicuous, as reflected by the values of $O_{alkoxido}$–Mn–$O_{alkoxido}$ [78.25(7)–82.34(7)°, average 80.5(1)°] and Mn–$O_{alkoxido}$–Mn [96.55(7)–101.41(7)°, average 98.9(1)°]. The face diagonal Mn···Mn vectors in the cluster reflect the different Mn–$O_{alkoxido}$ bond lengths, with the Mn1···Mn3 [3.249(1) Å] and Mn1···Mn2 [3.394(2) Å] distances being the longest and the shortest, respectively. The shortest Mn···Mn distance corresponds to the smallest Mn–O–Mn [96.78(7)°] and the largest O–Mn–O [82.34(7)°] internal cube angles, whereas the longest Mn···Mn distance corresponds to the larger Mn–O–Mn [101.41(7)°] and the smaller O–Mn–O [78.71(7)°] angles. The Mn–O_{ether}, Mn–$O_{alkoxido}$, and Mn–$O_{hydroxido}$ bonds lie well within the range of reported values for the corresponding bond lengths in other manganese(II) compounds.[1g] The deformation of the coordination geometry around the metal center was analyzed in terms of the continuous shape measures.[4] The values of the metric shape parameters (Table S1, Supporting Information) indicated that coordination surrounding each manganese ion can be described as an octahedron distorted towards a trigonal prism. The centrosymmetric structure of **2** is composed of four manganese cations, two bromide anions, and eight 2-methoxyethanolate anions (Figure 2). The manga-

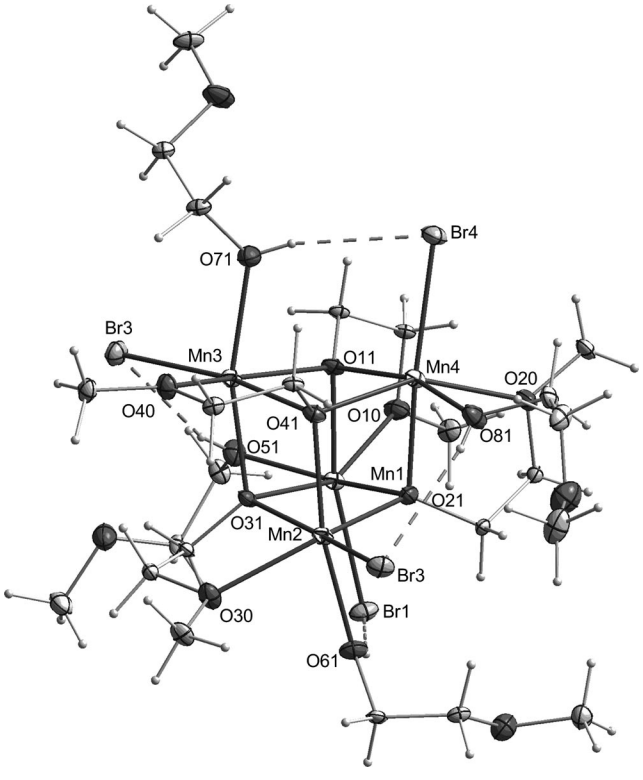

Figure 1. Molecular structure of **1** with hydrogen atoms omitted. Selected bond lengths [Å]: Mn1–O11 2.184(2), Mn1–O21 2.193(2), Mn1–O31 2.163(2), Mn2–O11 2.202(2), Mn2–O21 2.197(2), Mn2–O41 2.150(2), Mn3–O21 2.161(2), Mn3–O31 2.183(2), Mn3–O41 2.208(2), Mn4–O11 2.168(2), Mn4–O31 2.211(2), Mn4–O41 2.179(2), Mn1···Mn3 3.249(1),Mn1···Mn2 3.394(2), Mn1···Mn4 3.279(1), Mn2···Mn3 3.279(1), Mn2···Mn4 3.280(1), Mn3···Mn4 3.388(2).

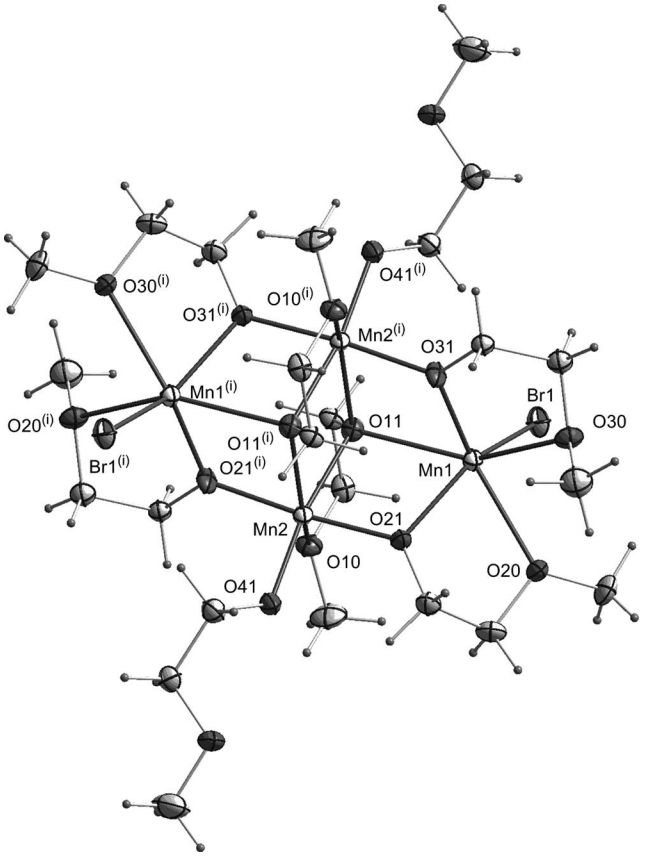

Figure 2. Molecular structure of **2** with hydrogen and disordered carbon atoms omitted. Selected bond lengths [Å]: Mn1–O11 2.379(2), Mn1–O21 2.062(2), Mn1–O31 2.085(2), Mn2–O11 2.007(2), Mn2–O21 1.906(2), Mn2–O41 1.847(2), Mn2–$O11^{(i)}$ 2.246(2), Mn2–$O31^{(i)}$ 1.912(2), Mn1···Mn2 3.281(2), Mn1···$Mn2^{(i)}$ 3.381(1), Mn2···$Mn2^{(i)}$ 3.335(1). Symmetry operation: $^{(i)}$ $-x + 1$, $-y$, $-z + 2$.

nese ions and bridging alkoxido groups are arranged in a face-shared dicubane-like core with two missing vertices. The planar Mn_4 rhombus can be described as being composed of two Mn_3 triangular faces, each held together by a μ_3-oxygen atom [O11 or O11$^{(i)}$] of a $CH_3OCH_2CH_2O^-$ ligand. The external edges of each triangle are hold by μ_2-oxygen atoms [O21] and [O31]. The stoichiometry of the complex requires that the average oxidation level for the manganese atoms is 2.5. The structural data provide strong evidence for the localization of the charges; bond lengths around Mn2 are significantly shorter than equivalent bonds to Mn1. On the basis of charge balance considerations, bond valence sum analysis (BVS),[5] DFT calculations,[6] and the presence of Jahn–Teller axial elongations at Mn, it has been assumed that the diagonal Mn2 center is in the trivalent state, whereas the Mn1 ion is divalent (Table S2, Supporting Information). The analysis of the coordination polyhedra of the manganese ions in these complexes indicated that Mn^{III} ions can be roughly described as octahedra with some degree of trigonal distortion, whereas the Mn^{II} are much closer to the trigonal prism (Table S1, Supporting Information).[4] Such a deviation of the metal coordination spheres can be attributed mostly to the combined effects of a chelating distortion (Mn1) and Jahn–Teller effect (Mn2). The Jahn–Teller distortion of the manganese center is approximately parallel to the bridging $Mn^{III}_2O_2$ plane. As a result of this, the Mn^{III}–O–Mn^{III} angle [103.12(2)°] is the largest one observed to date for such a system.[7] The intramolecular Mn···Mn distances change from 3.281(2) to 3.381(1) Å and are related to the oxidation states of manganese atoms. It was found that one of the $CH_3OCH_2CH_2O^-$ ligands coordinated to the divalent center (Mn1) is statistically distorted between two positions. The presence of electronic interaction between the manganese ions is indicated by magnetic measurements.

Magnetochemistry

The magnetic susceptibility was measured under a magnetic field of 500 mT in the temperature range 1.8–300 K. Diamagnetic corrections (–582 and -485×10^{-6} emu mol^{-1} for **1** and **2**, respectively) were calculated by using Pascal's constants. The magnetic susceptibility of **1** obeys the Curie–Weiss law above 100 K, with a Weiss constant θ = +15.9 K and a magnetic moment of 11.09 μ_B, which is a little less than the value of 11.83 μ_B (g = 2.00) expected for an uncoupled Mn^{II}_4 system with $S_{Mn}{}^{II}$ = 5/2. The effective magnetic moment [$\mu_{eff} = 2.828(\chi T)^{1/2}$] increases from 6.1 μ_B at 1.9 K, achieves a maximum at 30 K (12.5 μ_B), and then slowly decreases to 11.4 μ_B at 300 K (Figure 3). The increase in the moment with a decrease in the temperature suggests ferromagnetic interaction between some pairs of Mn^{II} ions, and the drop at low temperature implies the presence of an antiferromagnetic component in the total spin exchange.

To fit the experimental data the Kambe vector coupling method was applied. Even though the exact symmetry of the Mn^{II}_4 cluster is low, the reasonable simplifying approximation is possible by taking equal Mn1–Mn2 [d(Mn–Mn) = 3.394(2) Å] and Mn3–Mn4 [d = 3.388(2) Å] magnetic interactions with the coupling constant J_1, and Mn1–Mn3, Mn1–Mn4, Mn2–Mn3, and Mn2–Mn4 [d = 3.249(2)–3.280(1) Å] with J_2 (see Figure 1 for the definition of atom numbers). The Heisenberg spin Hamiltonian can be written as: = $-2J_1(\mathbf{S}_1\cdot\mathbf{S}_2 + \mathbf{S}_3\cdot\mathbf{S}_4) - 2J_2(\mathbf{S}_1\cdot\mathbf{S}_3 + \mathbf{S}_1\cdot\mathbf{S}_4 + \mathbf{S}_2\cdot\mathbf{S}_3 + \mathbf{S}_2\cdot\mathbf{S}_4)$, where $\mathbf{S}_i$ is the spin of the Mn ion number i. The good fit of the experimental μ_{eff} data to the theoretical model (Figure 3) was obtained with J_1 = 1.2 cm^{-1}, J_2 = –0.10 cm^{-1}, g = 2.00 (fixed), the temperature independent paramagnetism (TIP) fixed at 0, and intermolecular interaction zJ' = –0.090 cm^{-1} (the agreement factor $R = \Sigma[(\chi T)_{exp.} - (\chi T)_{calcd.}]^2/\Sigma\,[(\chi T)_{exp.}]^2 = 2.0\times10^{-3}$). No significant improvement in the fit was achieved after employing a spin Hamiltonian with more than two different coupling constants and/or an axial zero-field splitting parameter D (using the program julX written by E. Bill[8]).

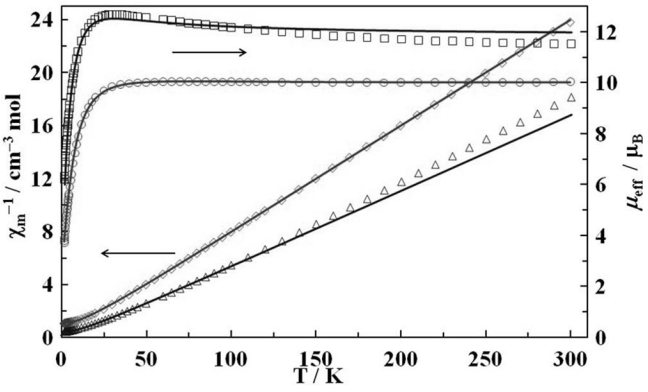

Figure 3. Variation of χ^{-1} (triangles – **1**, diamonds – **2**) and μ_{eff} (squares – **1**, circles – **2**) with temperature. The solid lines represent the best fit of the data (see text for details).

The appearance of ferromagnetic coupling between the Mn^{II} ions in **1** is rather unexpected, although ferromagnetic exchange is sometimes observed in Mn^{II} dimers with oxide,[9] chloride,[10] and nitride[11] bridges. Contrary to the iron(III) complexes containing Fe^{III}–O–Fe^{III} bridges, where the average Fe–O distances (and not the Fe–O–Fe bridging angles) are correlated with the exchange coupling constants,[12] analogical relationships in the isoelectronic Mn^{II} compounds have not been found. It was only noticed that the presence of N-donor terminal ligands favors ferromagnetic coupling.[10a]

Mn^{II}_4 clusters with a cubane topology are sparse.[1e,1h,13] All of them exhibit an antiferromagnetic coupling of the spins and monotonically increasing effective magnetic moment (or χT) with the temperature. In comparison with previously investigated cubane-like Mn^{II}_4 compounds, complex **1** has the most compact [$Mn_4(\mu_3\text{-}O)_4$] core with very short average Mn–O_{bridge} [2.183(2) Å] and Mn–Mn distances [3.312(2) Å]. This fact would support an assumption that short Mn–O and Mn–Mn distances favor ferromagnetic exchange interactions between the Mn^{II} ions. It is worth noting that only the nonlinear Mn^{II} tetramer with intra-

molecular ferromagnetic interactions, which consists of the centered trigonal Mn[(μ-phenoxido)$_2$Mn]$_3$ core, has even shorter average d(Mn–O_{bridge}) = 2.152 Å and d(Mn–Mn) = 3.27 Å.[14]

The magnetic susceptibility of complex **2** is plotted as χ^{-1} and the effective magnetic moment of a tetranuclear molecule versus T in Figure 3. In the range 150–300 K, the susceptibility obeys the Curie–Weiss law with a Weiss constant θ = –1.8 K and a magnetic moment of 10.05 μ_B, which is a little less than the value of 10.88 μ_B (g = 2.00) expected for an uncoupled $Mn^{II}_2Mn^{III}_2$ system with $S_{Mn^{II}}$ = 5/2 and $S_{Mn^{III}}$ = 2 local spins. The effective magnetic moment increases from 3.7 μ_B at 1.8 K to 10.0 μ_B in the 40–300 K region. The best fit of the data ($R = 2.8 \times 10^{-5}$, 66 points) led to J_{bb} = 3.9 cm^{-1}, J_{wb} = –0.35 cm^{-1}, g = 1.82, temperature independent paramagnetism (TIP) fixed at 600×10^{-6} cm^3 mol^{-1} [$\boldsymbol{H} = -2J_{bb}(\mathbf{S}_{Mn2}\mathbf{S}_{Mn2A}) - 2J_{wb}(\mathbf{S}_{Mn1} + \mathbf{S}_{Mn1A})(\mathbf{S}_{Mn2} + \mathbf{S}_{Mn2A})$].[2g] The ground-state spin S_T was found to be 1, and no SMM behavior was observed. The first 14 levels are all within 10 cm^{-1} of the ground state. The g value must be taken with caution, as this parameter reflects most of the experimental artifacts.[13b,15] The fact that the S_T = 1 level is lowest in **2** is uncommon at first sight, but may be explained with the aid of magnetostructural correlations. The comparison of magnetic and some structural data of compounds containing a $Mn^{II}_2Mn^{III}_2$ system shows a dependence between these parameters, as presented in Figure 4 (Table 1). The magnetic exchange interactions between the Mn ions are ferromagnetic in most of the compounds containing a tetrameric $Mn^{II}_2Mn^{III}_2$ center, giving a maximum allowable value of S_T = 9. For these compounds, the Jahn–Teller axes are parallel to the $Mn^{III}_2O_2$ plane, with d(Mn^{III}–Mn^{III}) > 3.1 Å and two different Mn^{III}–O distances in the bridge: 1.97 and 2.24 Å on average (Table 1). The Mn^{III}–O–Mn^{III} angle is in the range 97–103°. Along with increasing this angle, ferromagnetic interactions J_{bb} and J_{wb} decrease, and the last parameter achieves even negative values.

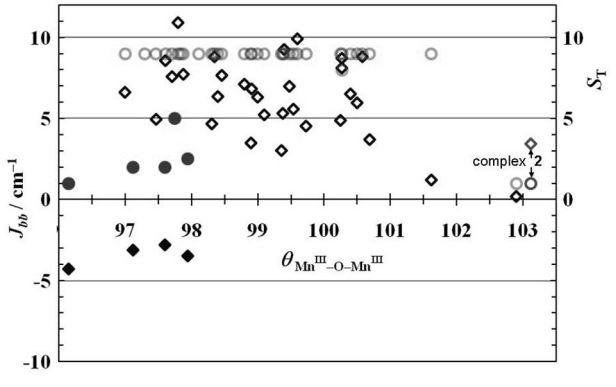

Figure 4. Correlation between J_{bb} (diamonds), S_T (circles) and Mn^{III}–O–Mn^{III} bridging angle for complexes containing rhomboidal $Mn^{II}Mn^{III}_2Mn^{II}$ central unit. Full symbols represent compounds with Jahn–Teller distortion perpendicular to the [Mn^{III}(μ-O)]$_2$ plane. See Table 1 for details and the Supporting Information for additional discussion.

Such conditions favor orbital overlap and thus increase the antiferromagnetic component of this magnetic interaction. Compound **2** with the Mn2–O11–Mn2^i angle equal to 103.12(8)° and large Mn^{III}–Mn^{III} distance 3.335(1) Å belongs to this class. The closest analog of **2** is [Mn_4(μ_3,η^2-hmp)$_2$(μ,η^2-hmp)$_4$(η^2-hmpH)$_2$] (ClO_4)$_4$·2MeCN (Hhmp: 2-hydroxymethylpyridine), with very similar dimensions of the central unit (Table 1) and S_T = 1 ground-state spin.[25]

Computational Results

To extract information about the site of oxidation, single-point DFT calculations for **2** as described in the Supporting Information were performed (Scheme 2). The values of both the charges and the spin polarization indicate that Mn1 is in the divalent state and Mn2 is trivalent. This is particularly noticeable when the spin polarizations are taken into account: five unpaired electrons at Mn1 site and four at Mn2. The Mulliken charges are lower than expected for ideally ionic bonds, indicating thus a significant overlapping of the 3d orbitals of Mn with those of the closest neighbors and, in consequence, a partially covalent character of the Mn–O,Br bonds. The HOMO (Figure S3, Supporting Information) is composed of approximately 50% 3d functions of Mn1 and the rest of the contribution comes from a few percent shares of neighboring O atoms, Mn2, and Br, the last being the greatest (approx. 9%). The previous orbital (HOMO-1), located a few hundred (500 for the calculations with the PW91 functional and 700 for the BLYP) cm^{-1} below, contains ca. 30% of the 3d functions of Mn2 and a less significant admixture (10–12%) of 3d orbitals of Mn1; the rest is composed mostly of the 2p functions of neighboring oxygen atoms. The LUMO, contrary to the HOMO, has a significant share (more than 50%) of the 3d orbitals of Mn2. In this way the energy gap between the highest occupied and the lowest unoccupied states with dominant share of Mn2 orbitals is approximately 14100 (PW91) or 14200 (BLYP) cm^{-1}. The analogous gap for Mn1 is much greater and may be estimated as 31000 cm^{-1} [a few hundred (500 for the calculations with the PW91 functional and 700 for the BLYP) cm^{-1} below, contains ca. 30% of the 3d functions of Mn2 and a less significant admixture (10–12%) of 3d orbitals of Mn1; the rest is composed mostly of the 2p functions of neighboring oxygen atoms].

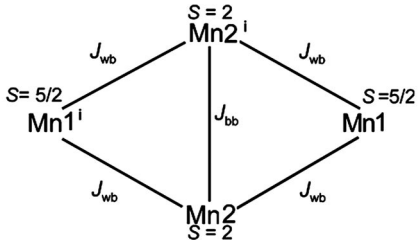

Scheme 2. Possible Mn···Mn magnetic interactions in **2**.

Table 1. Parameters of exchange coupling for compounds containing rhomboidal $Mn^{II}_2Mn^{III}_2$ system. θ denotes the Mn^{III}–O–Mn^{III} angle, d the Mn^{III}–Mn^{III} distance, g the Landé splitting factor, J_{bb} and J_{wb} the magnetic exchange parameters between Mn^{III}···Mn^{III} and Mn^{III}···Mn^{II} pairs, and S_T the ground-state spin.

	θ / °	d / Å	g	J_{bb} / cm^{-1}	J_{wb} / cm^{-1}	S_T	Ref.
$[Mn_4O_2(O_2CMe)_2(L^1)_2]^{2-}$[a]	96.2	2.798	1.80	–4.3	–3.9	1	[16]
$[Mn_4(teaH_2)_2(teaH)_2(PhCO_2)_2]^{2-}$	97.0	3.165	1.95	6.6	0.40	9	[2d]
$[Mn_4O_2(O_2CMe)_6(bipy)_2]$[a]	97.1	2.779	1.70	–3.1	–1.97	2	[17]
$[Mn_4(HL^2)_4(MeOH)_4Br_2]$	97.3	3.244	1.89	12.5	3.25	9	[18]
$[Mn_4(hmp)_4(OH)_2Mn(dcn)_6]$	97.5	3.172	1.95	4.9	1.04	9	[19]
$[Mn_4O_2(O_2CCPh_3)_6(OEt_2)_2]$[a]	97.6	2.770	1.47	–2.8	–1.5	2	[20]
$[Mn_4(team)_2(teaH_2)_2(O_2CPh)_2]^{2-}$	97.6	3.174	1.95	8.6	1.8	9	[1i]
$[Mn_4(hmp)_4Br_2(OMe)_2(dcn)_2]$	97.7	3.160	1.98	7.6	0.90	9	[2c]
$[Mn_4O_2(cao)_4(MeCN)_2(H_2O)_6]^{2-}$[a]	97.8	2.773	1.88	–46.0	–2.50	5	[21]
$[Mn_4(teaH_2)_2(teaH)_2(EtCO_2)_2]^{2-}$	97.8	3.187	1.95	10.9	0.22	9	[2d]
$[Mn_4(O_2CPh)_4(mda)_2(mdaH)_2]$	97.8	3.166	1.78			9	[22]
$[Mn_4(HL^2)_4(MeOH)_4Cl_2]$	97.9	3.281	1.89	7.7	3.42	9	[18]
$[Mn_4O_2(O_2CCHMe)_6(bpm)_2(EtOH)_4]$[a]	98.0	2.800	2.00	–3.5	–1.74	2.5	[23]
$[Mn_4(hmp)_6Cl_2]^{2-}$	98.1	3.215				9	[24]
$[Mn_4(idea)_2(bdeaH)_2(O_2CCMe_3)_4]$	98.3	3.162	1.97	4.7	0.28	9	[1i]
$[Mn_4(hmp)_6(dcn)_2]^{2-}$	98.4	3.189	1.98	6.3	0.71	9	[2c]
$[Mn_4(hmp)_6Br_2(H_2O)_2]^{2-}$	98.4	3.192	1.94	8.8	0.93	9	[2g]
$[Mn_4(bdea)_2(bdeaH)_2(O_2CPh)_4]$	98.5	3.174	2.00	7.6	0.90	9	[1i]
$[Mn_4(hmp)_6(H_2O)_2(NO_3)_2]^{2-}$	98.8	3.230	1.96	7.1	0.80	9	[2b]
$[Mn_4(hmp)_6(NO_3)_2(dcn)_2]$	98.9	3.210	1.94	6.8	1.12	9	[2c]
$[Mn_4(hmp)_6(H_2O)_4]^{4-}$	98.9	3.230	2.01	3.5	0.38	9	[25]
$[Mn_4(hmp)_6(NO_3)_4]$	99.0	3.207	1.99	6.3	4.2	9	[26]
$[Mn_4(hmp)_6(PhCO_2)_2(H_2O)_2]^{2-}$	99.1	3.220	2.01	5.2	0.90	9	[27]
$[Mn_4(hmp)_6(MeCN)_2]^{4+}$	99.4	3.187	1.99	3.0	0.43	9	[28]
$[Mn_4(hmp)_4(acac)_2(MeO)_2]^{2-}$	99.4	3.202	1.93	5.3	0.78	9	[26]
$[Mn_4(hmp)_6(H_2O)_2(NO_3)_2]^{2-}$	99.4	3.253	1.93	9.2	0.86	9	[25]
$[Mn_4(hmp)_6(MeCN)_2]^{4+}$	99.5	3.211	2.02	7.0	0.40	9	[28]
$[Mn_4(hmp)_6(MeCO_2)_2(H_2O)_2]^{2-}$	99.5	3.218	1.94	5.6	0.54	9	[27]
$[Mn_4(hmp)_6(NO_3)_2(MeCN)_2]^{2-}$	99.6	3.228	1.87	9.9	1.0	9	[26]
$[Mn_4(hmp)_6(MeCO_2)_2]^{2-}$	99.7	3.211	1.94	4.5	1.3	9	[27]
$[Mn_4(hmp)_6(ClCH_2CO_2)_2]^{2-}$	100.3	3.234	1.98	4.9	1.1	9	[27]
$[Mn_4(O_2CMe)_2(pdmH)_6]^{2-}$	100.3	3.253	1.84	8.1	0.40	8	[29]
$[Mn_4(O_2CMe)_2(pdmH)_6]^{2-}$	100.3	3.253	1.89	8.7	1.1	9	[29]
$[Mn_4(teaH_2)_2(teaH)_2(H_2O)_2(MeCO_2)_2]^{2-}$	100.4	3.222	1.89	6.5	1.7	9	[2d]
$[Mn_4(hmp)_6(MeCN)_2(H_2O)_4]^{4-}$	100.5	3.235	1.96	5.9	0.46	9	[30]
$[Mn_4(hmp)_4(pdmH)_2(dcn)_2]^{2-}$	100.6	3.238	1.97	8.8	0.80	9	[2c]
$[Mn_4(hmp)_6(CCl_3CO_2)_2(H_2O)_2]^{2-}$	100.7	3.237	1.99	3.7	0.69	9	[27]
$[Mn_4(N_3)_4(pdmH)_2(team)_2]$	101.6	3.267	1.96	1.2	0.03	9	[31]
$[Mn_4(hmp)_6(hmpH)_2]^{4-}$	102.9	3.353	2.05	0.2	–0.64	1	[25]
$[Mn_4Br_2(OCH_2CH_2OCH_3)_8]$	103.1	3.335	1.83	3.4	–0.36	1	this work

[a] Jahn–Teller distortion perpendicular to the $[Mn^{III}(\mu_2\text{-}O)]_2$ plane. Abbreviations: acac = 2,4-pentanedione; $bdeaH_2$ = *N*-butyldiethanolamine; bipy = bipyridine; bpm = 2,2′-bipyrimidine; caoH = HON = C(CN)CONH$_2$; dcn$^-$ = N(CN)$_2^-$; hmpH = 2-hydroxymethylpyridine; L^1 = 1,2-bis(bipyridine-6′-yl)ethane; H_3L^2 = 2,6-bis(hydroxymethyl)-4-methylphenol; $mdaH_2$ = *N*-methyldiethanolamine; $pdmH_2$ = pyridine-2,6-dimethanol; $teaH_3$ = triethanolamine.

Conclusions

In conclusion, in a one-step reaction we have synthesized two different tetranuclear manganese species and shown which factors play a role in the formation of each of them. Complex **2** is a mixed-valent species containing two Mn^{III} and two Mn^{II} ions. Given that the starting manganese source contains only metallic manganese it is clear that the Mn^{II} ions are formed directly by oxidation of Mn by HBr. The Mn^{III} ions are formed by aerial oxidation[10] of Mn^{II} during stirring of the reaction mixture because of inadvertent exposure to air during stirring or by MnO_2. The formation of two chemically and structurally different tetranuclear units can be explained in terms of the geometric requirements resulting from ligand field theory and the influence of ligands. The Mn^{II} ion with d^5 has no particular preference for geometry, whereas the d^4 configuration of Mn^{III} enforces a more rigid geometry. When the manganese ion is oxidized to the +3 state, its geometry stiffens and this reduces the angular lability at that center. At this stage of the oxidation process the system has some conformational flexibility, and the diagonally opposite manganese ion is oxidized next. As before, the oxidation is accompanied by a geometric rearrangement in which the angular geometry of the +3 ion is ordered. All these changes are transmitted through the ligand framework to the remaining +2 ions. The more rigorous geometric requirements enforced by the +3 ions reduce the mobility of the system at each oxidation step. In the case of manganese, the irregular geometry imposed on the remaining two +2 metal ion sites (which is stabilized by bromide ion) is sufficient to move their redox

potential out of the range accessible for the system, yielding, in effect, a mixed-valence $Mn^{II}_2Mn^{III}_2$ complex. In the case of **1**, ligand-ligand interactions such as hydrogen bonds are important factors in stabilizing the cuboidal $[Mn_4(\mu_3\text{-}O)_4]$ core.

Experimental Section

Synthesis: All reactions were conducted under a nitrogen atmosphere. Chemicals were treated as follows: toluene, distilled from Na/benzophenone; hexanes, distilled from P_2O_5; and 2-methoxyethanol (Aldrich), distilled prior to use. Metallic Mn and NH_4Br (Aldrich) were used as received. Microanalyses were conducted with an ASA-1 (GDR, Karl–Zeiss–Jena) instrument (in-house).

Method A: To a suspension of NH_4Br (2.34 g, 23.8 mmol) in a mixture of $CH_3OCH_2CH_2OH$/toluene (40:10 mL) was added metallic manganese (1.31 g, 23.8 mmol). The mixture was heated under reflux until the evolution of NH_3 had ceased (48 h). The resulting dark-brown slurry was filtered, and the filtrate was left to crystallize. After a few days, colorless crystals of $[Mn_4(\mu_3,\eta^2\text{-}L)_4Br_4(LH)_4]$ (**1**, 62.04%) were collected by filtration. $C_{24}H_{60}Br_4Mn_4O_{16}$ (1144.10): calcd. C 25.20, H 5.29, Br 27.94, Mn 19.21; found C 25.16, H 5.20, Br 28.03, Mn 19.17. The filtrate was concentrated to ca. 20 mL and kept at room temperature for a few days. It slowly yielded red crystals of $[Mn_4(\mu_3,\eta^2\text{-}L)_2(\mu,\eta^2\text{-}L)_4L_2Br_2]$ (**2**, 8.40%). $C_{24}H_{56}Br_2Mn_4O_{16}$ (980.26): calcd. C 25.20, H 5.29, Br 27.94, Mn 19.21; found C 25.01, H 5.21, Br 27.73, Mn 19.28.

Method B: To a suspension of NH_4Br (2.42 g, 24.7 mmol) and MnO_2 (0.59 g, 6.79 mmol) in a mixture of $CH_3OCH_2CH_2OH$/toluene/thf (30:10:10 mL) was added metallic manganese (1.36 g, 24.7 mmol), and the mixture was heated for 3 d under reflux. Colorless crystals of $[Mn_4(\mu_3,\eta^2\text{-}L)_4Br_4(LH)_4]$ (**1**) were collected by filtration. The filtrate was concentrated to ca. 20 mL and after a few days at room temperature red crystals of $[Mn_4(\mu_3,\eta^2\text{-}L)_2(\mu,\eta^2\text{-}L)_4L_2Br_2]$ (**2**) were formed. The crystals were filtered off and dried in vacuo (28.90%).

Table 2. Crystal data and structure refinement for **1** and **2**.

	1	**2**
Empirical formula	$C_{24}H_{60}Br_4Mn_4O_{16}$	$C_{24}H_{56}Br_2Mn_4O_{16}$
Formula weight	1144.12	980.27
Temperature / K	100(2)	100(2)
Wavelength / Å	0.71073	0.71073
Crystal system	monoclinic	monoclinic
Space group	$P2_1/n$	$P2_1/c$
a / Å	18.134(5)	11.481(5)
b / Å	12.883(4)	20.407(6)
c / Å	19.284(5)	8.094(4)
β / °	107.46(3)	92.20(2)
Volume / Å^3	4298(2)	1895(2)
Abs. coefficient / mm^{-1}	4.93	3.47
F(000)	2288	996
Crystal size / mm	$0.38\times0.23\times0.09$	$0.21\times0.19\times0.09$
θ range for data collection	3.1, 28,1	2.7, 27.5
Reflections collected	58608	18376
Independent reflections	10393	4336
R_{int}	0.051	0.072
Data, restraints, parameters	10393, 0, 457	4336, 0, 220
Goodness-of-fit on F^2	1.11	0.83
R_1, wR_2[a] [$I>2\sigma(I)$]	0.034, 0.055	0.031, 0.046
R_1, wR_2[a] (all data)	0.048, 0.058	0.071, 0.051
$\Delta\rho_{max}$, $\Delta\rho_{min}$ / e Å^{-3}	0.39, –0.40	0.53, –0.39

[a] $R_1 = \Sigma||F_o| - |F_c||/\Sigma|F_o|$; $wR_2 = [\Sigma w(F_o^2 - F_c^2)^2/\Sigma w(F_o^2)^2]^{1/2}$.

Crystal Structure Determination: Crystals were mounted on glass fibers and then flash-frozen to 100(2) K (Oxford Cryosystem-Cryostream Cooler; Table 2). Preliminary examination and intensity data collections were carried out with a Kuma KM4CCD κ-axis diffractometer with graphite-monochromated Mo-K_α radiation. All data were corrected for Lorentz, polarization, and absorption effects. Data reduction and analysis were carried out with the Kuma Diffraction programs.[32] All structures were solved by direct methods and refined by the full-matrix least-squares method on all F^2 data by using the SHELXTL software.[33] Carbon-bonded hydrogen atoms were included in calculated positions and refined in the riding mode by using SHELXTL default parameters. Other hydrogen atoms were located in a difference map. In **2** one of coordinated $CH_3OCH_2CH_2O^-$ molecules was found to be disordered over two positions (0.50:0.50). Continuous shape measure analysis for coordination sphere of Mn were performed with the use of SHAPE v. 1.1b software.[4] (Table S1, Supporting Information). Bond valence sum analysis were performed with use of VaList v.3.0.17 software[34] (Table S2, Supporting Information).

CCDC-757981 (for **1**) and -757982 (for **2**) contain the supplementary crystallographic data for this paper. These data can be obtained free of charge from The Cambridge Crystallographic Data Centre via www.ccdc.cam.ac.uk/data_request/cif.

Supporting Information (see footnote on the first page of this article): Tables giving descriptors of CSM analysis, bond valence calculations, and DFT calculations; figures showing, magnetic properties and DFT calculations.

Acknowledgments

This work was supported by the Polish Ministry of Science and Higher Education for Scientific Research (Grants N205 4036 33 and N204 1527 38). The ADF calculations were carried out at the Wrocław Centre for Networking and Supercomputing (Grant No. 58).

[1] a) O. Roubeau, R. Clérac, *Eur. J. Inorg. Chem.* **2008**, 4325; b) K. L. Taft, A. Caneschi, L. E. Pence, C. D. Delfs, G. C. Papaefthymiou, S. J. Lippard, *J. Am. Chem. Soc.* **1993**, *115*, 11753; c) A. F. Williams, *Dalton Trans.* **2008**, 818; d) C. C. Beedle, K. J. Heroux, M. Nakano, A. G. DiPasquale, A. L. Rheingold, D. N. Hendrickson, *Polyhedron* **2007**, *26*, 2200; e) M. L. Tong, S. L. Zheng, J. X. Shi, Y. X. Tong, H. K. Lee, X. M. Chen, *J. Chem. Soc., Dalton Trans.* **2002**, 1727; f) M. Nihei, N. Hoshino, T. Ito, H. Oshio, *Chem. Lett.* **2002**, 1016; g) L. B. Jerzykiewicz, J. Utko, M. Duczmal, P. Sobota, *Dalton Trans.* **2007**, 825; h) G. S. Papaefstathiou, A. Escuer, F. A. Mautner, C. Raptopoulou, A. Terzis, S. P. Perlepes, R. Vicente, *Eur. J. Inorg. Chem.* **2005**, 879; i) A. M. Ako, V. Mereacre, I. J. Hewitt, R. Clerac, L. Lecren, C. E. Anson, A. K. Powell, *J. Mater. Chem.* **2006**, *16*, 2579; j) L. Stelzig, A. Steiner, B. Chansou, J.-P. Tuchagues, *Chem. Commun.* **1998**, 771; k) Y. Sunatsuki, H. Shimada, T. Matsuo, M. Nakamura, F. Kai, N. Matsumoto, N. Re, *Inorg. Chem.* **1998**, *37*, 5566.

[2] a) S. Mukhopadhyay, S. K. Mandal, S. Bhaduri, W. H. Armstrong, *Chem. Rev.* **2004**, *104*, 3981; b) L. Lecren, W. Wernsdorfer, Y.-G. Li, O. Roubeau, H. Miyasaka, R. Clérac, *J. Am. Chem. Soc.* **2005**, *127*, 11311; c) H. Miyasaka, K. Nakata, L. Lecren, C. Coulon, Y. Nakazawa, T. Fujisaki, K. Sugiura, M. Yamashita, R. Clérac, *J. Am. Chem. Soc.* **2006**, *128*, 3770; d) L. M. Wittick, K. S. Murray, B. Moubaraki, S. R. Batten, L. Spiccia, K. J. Berry, *Dalton Trans.* **2004**, 1003; e) E. K.

Brechin, J. Yoo, M. Nakano, J. C. Huffman, D. N. Hendrickson, G. Christou, *Chem. Commun.* **1999**, 783; f) L. M. Wittick, L. F. Jones, P. Jensen, B. Moubaraki, L. Spiccia, K. J. Berryb, K. S. Murray, *Dalton Trans.* **2006**, 1534; g) J. Yoo, A. Yamaguchi, M. Nakano, J. W. Krzystek, E. Streib, L.-C. Brunel, H. Ishimoto, G. Christou, D. N. Hendrickson, *Inorg. Chem.* **2001**, *40*, 4604.

[3] a) J. E. Sheats, R. S. Czernuszewicz, G. C. Dismukes, A. L. Rheingold, V. Petrouleas, J. Stubbe, W. H. Armstrong, R. H. Beer, S. J. Lippard, *J. Am. Chem. Soc.* **1987**, *109*, 1435; b) R. L. Rardin, P. Poganiuch, A. Bino, D. P. Goldberg, W. B. Tolman, S. Liu, S. J. Lippard, *J. Am. Chem. Soc.* **1992**, *114*, 5240; c) R. Mukhopadhyay, S. Bhattacharjee, R. Bhattacharyya, *J. Chem. Soc., Dalton Trans.* **1994**, 2799; d) J. McCrea, V. McKee, T. Metcalfe, S. S. Tandon, J. Wikaira, *Inorg. Chim. Acta* **2000**, 297 220; e) S. Naskar, S. Biswas, D. Mishra, B. Adhikary, L. R. Falvello, T. Soler, C. H. Schwalbe, S. K. Chattopadhyay, *Inorg. Chim. Acta* **2004**, *357*, 4257; f) Y. Mikata, M. Wakamatsu, H. So, Y. Abe, M. Mikuriya, K. Fukui, S. Yano, *Inorg. Chem.* **2005**, *44*, 7268; g) Y. Gultneh, Y. T. Tesema, T. B. Yisgedu, R. J. Butcher, G. B. Wang, G. T. Yee, *Inorg. Chem.* **2006**, *45*, 3023.

[4] a) H. Zabrodsky, S. Peleg, D. Avnir, *J. Am. Chem. Soc.* **1992**, *114*, 7843; b) M. Llunell, D. Casanova, J. Cirera, J. M. Bofill, P. Alemany, S. Alvarez, M. Pinsky, D. Avnir, *SHAPE*, v1.1b, University of Barcelona, Barcelona, Spain, **2005**.

[5] I. D. Brown, *Chem. Rev.* **2009**, *109*, 6858.

[6] ADF2005.01, SCM, Theoretical Chemistry, Vrije Universiteit, Amsterdam, The Netherlands; http://www.scm.com.

[7] Cambridge Crystallographic Data Centre. "ConQuest 1.11" CSD 5.3, January **2009** Release.

[8] http://ewww.mpi-muelheim.mpg.de/bac/logins/bill/julX_en.php.

[9] a) D. Luneau, J. M. Savariault, P. Cassoux, J. P. Tuchagues, *J. Chem. Soc., Dalton Trans.* **1988**, 1225; b) M. Wesolek, D. Meyer, J. A. Osborn, A. De Cian, J. Fischer, A. Derory, P. Logoll, M. Drillon, *Angew. Chem. Int. Ed. Engl.* **1994**, *4*, 1592; c) H. Wada, K. Motoda, M. Ohba, H. Sakiyama, N. Matsumoto, H. Okawa, *Bull. Chem. Soc. Jpn.* **1995**, *68*, 1105; d) A. Gelasco, M. L. Kirk, J. E. Kampf, V. L. Pecoraro, *Inorg. Chem.* **1997**, *36*, 1829.

[10] a) D. Armentano, G. de Munno, F. Guerra, J. Faus, F. Lloret, M. Julve, *Dalton Trans.* **2003**, 4626; b) I. Romero, M. N. Collomb, A. Deronzier, A. Llobet, E. Perret, J. Pécaut, L. L. Pape, J. M. Latour, *Eur. J. Inorg. Chem.* **2001**, 69.

[11] a) R. Cortes, J. L. Pizarro, L. Lezama, M. I. Arriortua, T. Rojo, *Inorg. Chem.* **1994**, *33*, 2697; b) Z. Xu, L. K. Thompson, D. O. Miller, H. J. Clase, J. A. K. Howard, A. E. Goeta, *Inorg. Chem.* **1998**, *37*, 3620.

[12] R. Werner, S. Ostrovsky, K. Griesar, W. Haase, *Inorg. Chim. Acta* **2001**, *326*, 78.

[13] a) J. Aussoleil, P. Cassoux, P. de Loth, J.-P. Tuchagues, *Inorg. Chem.* **1989**, *28*, 3051; b) L. E. Pence, A. Caneschi, S. J. Lippard, *Inorg. Chem.* **1996**, *35*, 3069; c) T. A. Hudson, K. J. Berry, B. Moubaraki, K. S. Murray, R. Robson, *Inorg. Chem.* **2006**, *45*, 3549; d) C. C. Stoumpos, I. A. Gass, C. J. Milios, E. Kefalloniti, C. P. Raptopoulou, A. Terzis, N. Lalioti, E. K. Brechin, S. P. Perlepes, *Inorg. Chem. Commun.* **2008**, *11*, 196; e) C. C. Stoumpos, I. A. Gass, C. J. Milios, N. Lalioti, A. Terzis, G. Aromí, S. J. Teat, E. K. Brechin, S. P. Perlepes, *Dalton Trans.* **2009**, 307; f) C. C. Stoumpos, N. Lalioti, I. A. Gass, K. Gkotsis, A. A. Kitos, H. Sartzi, C. J. Milios, C. P. Raptopoulou, A. Terzis, E. K. Brechin, S. P. Perlepes, *Polyhedron* **2009**, *28*, 2017.

[14] E.-Q. Gao, S.-Q. Bai, Z. He, C.-Hua Yan, *Inorg. Chem.* **2005**, *44*, 677.

[15] G. Aromí, P. Gamez, C. Boldron, H. Kooijman, A. L. Spek, J. Reedijk, *Eur. J. Inorg. Chem.* **2006**, 1940.

[16] E. C. Sañudo, V. A. Grillo, J. Yoo, J. C. Huffman, J. C. Bollinger, D. N. Hendrickson, G. Christou, *Polyhedron* **2001**, *20*, 1269; L. M. Wittick, K. S. Murray, B. Moubaraki, S. R. Batten, L. Spiccia, K. Berry, *Dalton Trans.* **2004**, 1003.

[17] J. B. Vincent, C. Christmas, H.-R. Chang, Q. Li, P. Boyd, J. C. Huffman, D. N. Hendrickson, G. Christou, *J. Am. Chem. Soc.* **1989**, *111*, 2086.

[18] C.-I. Yang, G.-H. Lee, C.-S. Wur, J. G. Lin, H.-L. Tsai, *Polyhedron* **2005**, *24*, 2215.

[19] H. Miyasaka, K. Nakata, K.-I. Sugiuara, M. Yamashita, R. Clérac, *Angew. Chem. Int. Ed.* **2004**, *43*, 707.

[20] H. H. Thorp, J. E. Sameski, R. J. Kulawiec, G. W. Brudvig, R. H. Crabtree, G. C. Papaefthymiou, *Inorg. Chem.* **1991**, *30*, 1153.

[21] D. J. Price, S. R. Batten, K. J. Berry, B. Moubaraki, K. S. Murray, *Polyhedron* **2003**, *22*, 165.

[22] D. Foguet-Albiol, T. A. O'Brien, W. Wernsdorfer, B. Moulton, M. J. Zaworotko, K. A. Abboud, G. Christou, *Angew. Chem. Int. Ed.* **2005**, *44*, 897.

[23] S. G. Baca, I. L. Malaestean, T. D. Keene, H. Adams, M. D. Ward, J. Hauser, A. Neels, S. Decurtins, *Inorg. Chem.* **2008**, *47*, 11108.

[24] J. Yoo, W. Wernsdorfer, E.-C. Yang, M. Nakano, A. L. Rheingold, D. N. Hendrickson, *Inorg. Chem.* **2005**, *44*, 3377.

[25] L. Lecren, O. Roubeau, C. Coulon, Y.-G. Li, X. F. Le Goff, W. Wernsdorfer, H. Miyasaka, R. Clérac, *J. Am. Chem. Soc.* **2005**, *127*, 17353.

[26] E. C. Yang, N. Harden, W. Wernsdorfer, L. Zakhrov, E. K. Brechin, A. L. Rheingold, G. Christou, D. N. Hendrickson, *Polyhedron* **2003**, *22*, 1857.

[27] L. Lecren, O. Roubeau, Y.-G. Li, X. F. Le Goff, H. Miyasaka, F. Richard, W. Wernsdorfer, C. Coulona, R. Clérac, *Dalton Trans.* **2008**, 755.

[28] H. Hiraga, H. Miyasaka, K. Nakata, T. Kajiwara, S. Takaishi, Y. Oshima, H. Nojiri, M. Yamashita, *Inorg. Chem.* **2007**, *46*, 9661.

[29] J. Yoo, E. K. Brechin, A. Yamaguchi, M. Nakano, J. C. Huffman, A. L. Maniero, L.-C. Brunel, K. Awaga, H. Ishimoto, G. Christou, D. N. Hendrickson, *Inorg. Chem.* **2000**, *39*, 3615.

[30] L. Lecren, Y.-G. Li, W. Wernsdorfer, O. Roubeau, H. Miyasaka, R. Clérac, *Inorg. Chem. Commun.* **2005**, *8*, 626.

[31] T. C. Stamatatos, K. M. Poole, K. A. Abboud, W. Wernsdorfer, T. A. O'Brien, G. Christou, *Inorg. Chem.* **2008**, *47*, 5006.

[32] Oxford Diffraction, *CrysAlis CCD* and *CrysAlis RED*, versions 1.171.31, Oxford Diffraction Poland, Wroclaw, Poland, **2006**.

[33] Bruker, *SHELXTL*, version 6.14, Bruker AXS Inc., Madison, Wisconsin, USA, **2003**.

[34] A. S. Wills, *VaList – Bond Valence Calculation and Listing*, v3.0.17, UCL London, England, **2008**.

Received: April 6, 2010
Published Online: August 16, 2010

